Nonlinear Elastic Viscous with Damage Model To Predict Permanent Deformation of Asphalt Concrete Mixes

JORGE SOUSA, SHMUEL L. WEISSMAN, JEROME L. SACKMAN, AND CARL L. MONISMITH

The development and use of a nonlinear elastic, viscous with damage model are discussed. The model is proposed as a constitutive relation for asphalt concrete mixes to permit prediction of permanent deformation. The model is intended to capture the macrobehavior of mixes, including (*a*) the dilatancy observed when the mix is subjected to shear strains, (*b*) the increase of effective shear modulus under increased hydrostatic pressure, (*c*) the significant variation of behavior with changes in temperature and rates of loading, and (*d*) the residual accumulation of permanent deformation under repetitive loading. This model has been developed as part of the Strategic Highway Research Program A-003A efforts to characterize the permanent deformation characteristics of asphalt-aggregate mixes. A new series of tests proposed for the determination of the material properties is presented, modeled and observed responses from a simple validation test are compared, and the use of the model to predict permanent deformation response in an asphalt concrete pavement section is illustrated.

This paper presents the results of a comprehensive investigation to characterize the permanent deformation behavior of asphalt concrete mixes as part of the Strategic Highway Research Program (SHRP) A-003A research program.

Research (*1–4*) has indicated that asphalt concrete demonstrates the following characteristics when subjected to rate-dependent loading over a range of temperatures: (*a*) it dilates under shear loading (i.e., there is a coupling between volumetric and deviatoric behaviors), (*b*) its effective shear modulus increases with increase in hydrostatic pressure, (*c*) it is temperature dependent, (*d*) it is rate dependent, (*e*) volumetric creep is negligible, and (*f*) residual permanent deformation is observed after the load has been removed (i.e., the material exhibits inelastic behavior).

Although most of these observations are not new, very little attention has been directed to the coupling between volumetric and deviatoric behavior and to the importance of deviatoric stresses. However, recent studies (*1*) suggest that permanent deformation is greatest in areas of high shear (near the edge of the tires). For this reason the present study emphasizes this coupling, which plays a significant role in the proposed model.

J. Sousa and C. L. Monismith, Institute of Transportation Studies, University of California at Berkeley, 1301 S. 46th St., Bldg. 452, Richmond, Calif. 94804. S. L. Weissman, Symplectic Engineering, 1350 Solano Avenue, No. 26, Albany, Calif. 94706. J. L. Sackman, Civil Engineering Department, University of California at Berkeley, 733 Davis Hall, Berkeley, Calif. 94720.

In the development of the model, the fact that dilatancy and hardening under hydrostatic pressure are typical of densely compacted aggregates was taken into the consideration. It was also recognized that aggregate behavior is not sensitive to temperature or loading rate, whereas asphalt/binder behavior is very sensitive to both temperature and rate of loading.

In the development of a comprehensive procedure to determine rutting in pavement sections, three aspects have to be considered:

1. Development and selection of a constitutive law that embodies the different aspects of the observed behavior of asphalt-aggregate mixes—recognizing that these mixes are not isotropic linear elastic materials (which can be fully characterized with a Young's modulus and a Poisson's ratio), the definition of a constitutive relationship incorporating the most important aspects of actual mix response is imperative;
2. Development and standardization of new test procedures to determine requisite parameters for the constitutive relationship—for linear elastic materials, determination of a Young's modulus and Poisson's ratio can be accomplished with a simple extension or compression test. On the other hand, determination of material parameters to define the responses of more complex materials requires several tests; and
3. Development of a finite element computer program that permits solution of boundary value problems using the constitutive relationship proposed for the asphalt-aggregate mix.

In this paper three aspects will be discussed: presentation of a constitutive relationship for asphalt-aggregate mixes together with a series of tests required to define the material parameters, preliminary validation of the constitutive relationship by comparing observed and predicted responses from a test other than those used to define the material properties, and use of the constitutive relationship to predict rutting propensity in an asphalt concrete pavement section.

PROPOSED CONSTITUTIVE LAW FOR ASPHALT CONCRETE

A nonlinear elastic viscous with damage constitutive relationship is proposed to represent the response of asphalt-aggregate mixes to stresses leading to permanent deformation. The model consists of a number of three-dimensional

Maxwell elements in parallel; each Maxwell element is composed of a nonlinear spring and dashpot. The dilatancy effect and the increase in effective shear modulus under hydrostatic pressure are due to the aggregate skeleton, whereas temperature and rate dependency are associated with the asphalt binder. Thus dilatancy and hardening are associated with the spring, and temperature and rate dependency are associated with the dashpot.

Consider first the spring in a typical Maxwell element. To achieve the desired coupling and hardening, the strain energy function is expanded in a Taylor series in terms of the strain invariants (i.e., the material is assumed to be initially isotropic) with truncation of terms of an order greater than four. Thus, the strain energy function is approximately (*5,6*)

$$W(\varepsilon^e) = \frac{1}{2} C_1 I_1^2 + C_2 I_2 + \frac{1}{3} C_3 I_1^3 + C_4 I_1 I_2 + C_5 I_3 + \frac{1}{4} C_6 I_1^4 + C_7 I_1^2 I_2 + C_8 I_1 I_3 + \frac{1}{2} C_9 I_2 \quad (1)$$

where

$C_1, C_2, \ldots C_9$ = material constants,
ε^e = elastic strain tensor, and
I_1, I_2, and I_3 = the elastic strain tensor invariants.

The term ε^e is a function of the total strain, ε, and the viscous (i.e., inelastic) strain, ε^i, given by (*5*)

$$\varepsilon^e = \varepsilon - \varepsilon^i \quad (2)$$

The stress tensor, ω, is defined as

$$\sigma = \delta_\varepsilon W(\varepsilon^e) \quad (3)$$

Second, consider the dashpot in a typical Maxwell element. In this case, the equilibrium equation is a rate equation of the following form (*7*):

$$\dot{\varepsilon}^i = \left(1 + \frac{q^n}{\alpha^n}\right) \eta^{-1} \delta_\varepsilon W(\varepsilon^e) \quad (4a)$$

or

$$\dot{\varepsilon}^i = \left(1 - \frac{q^n}{\alpha^n}\right)^{-1} \eta^{-1} \delta_\varepsilon W(\varepsilon^e) \quad (4b)$$

where α and n are material constants. The internal (damage) variable, q, is defined as

$$q = \max_{0 \le \tau \le t} (q_\tau) \quad (5)$$

and q_τ is given by

$$q_\tau = (\varepsilon^i : \varepsilon^i)_\tau^{1/2} \quad (6a)$$

when Equation 4b is used, and by

$$q_\tau = (\dot{\varepsilon}^i : \eta : \dot{\varepsilon}^i)_\tau^{1/2} \quad (6b)$$

when Equation 4a is used. In this expression η, the initial viscosity, is a Rank 4 tensor given in component form by

$$\eta_{ijkl} = \lambda^\nu \delta_{ij} \delta_{kl} + \mu^\nu (\delta_{ik} \delta_{jl} + \delta_{il} \delta_{jk}) \quad (7)$$

where λ^ν and μ^ν are the temperature-dependent material constants.

The thermorheologically simple nature of the asphalt concrete at small strains can be accommodated in the model if η is assumed to be

$$\eta = \eta_0 e^{\frac{C_T(T - T_0)}{T_0 T}} \quad (8)$$

where C_T is a material constant, T and T_0 are the current and reference temperature (in degrees Kelvin), respectively, and η_0 is given by Equation 7 with λ^ν and μ^ν evaluated at the reference temperature.

The two models proposed for Equation 4 differ in the definition of the "damage" parameter q (i.e., they differ in the evolution of the viscosity). The first model is based on the maximum attained strain, whereas the second is based on the maximum attained inelastic strain rate.

The global model is obtained when a number of nonlinear Maxwell elements are assembled in parallel. Note that all Maxwell elements share the same total strain, ε, whereas ε^e and ε^i are evaluated independently for each Maxwell element.

DETERMINATION OF MATERIAL PROPERTIES AND MODEL VALIDATION

Figure 1 shows the framework for permanent deformation prediction using the proposed constitutive equation. The de-

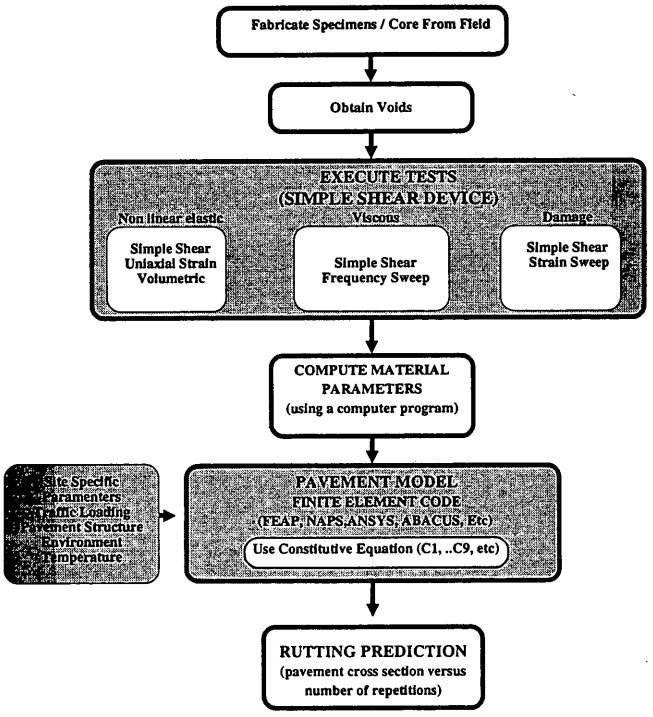

FIGURE 1 Framework to estimate permanent deformation in the asphalt concrete layer of a pavement structure.

termination of the material parameters is one of the first steps in the proposed procedure. It is accomplished by testing four cylindrical specimens 15 cm (6 in.) in diameter by 5 cm (2 in.) high.

With a finite element program capable of incorporating the appropriate constitutive equation for the asphalt concrete material and also constitutive equations for the other materials making up a pavement structure, predictions of rut depth can be made for given traffic and environment conditions.

To illustrate the efficacy of the procedure for permanent deformation determination to discriminate among different asphalt-aggregate combinations, mixes were selected containing Aggregates RB and RL and Asphalts AAK-1 and AAG-1 (materials from the SHRP Materials Reference Library). These mixes included

- V0W0—Aggregate RB, Asphalt AAG-1, low asphalt content, low void content;
- B0W0—Aggregate RB, Asphalt AAK-1, low asphalt content, low void content;
- B1T1—Aggregate RL, Asphalt AAK-1, high asphalt content, high void content; and
- V0T1—Aggregate RL, Asphalt AAG-1, low asphalt content, high void content.

Wheel-tracking tests had been performed by SWK/Nottingham on these mixes. Ranking in order of increasing normalized rutting rate was as follows (*8*): V0W0 < B0W0 < V0T1 < B1T1.

To permit comparisons, the following steps were followed:

1. The nonlinear elastic parameters were determined at 4°C (to minimize viscous effects).
2. The viscous parameters over a range of temperatures (4°C, 20°C, and 40°C) and frequencies (0.01, 0.02, 0.05, 0.1, 0.2, 0.5, 1.0, 2.0, 5.0, and 10 Hz) were determined.
3. The damage parameters were determined.
4. Using the Finite Element Analysis Program (FEAP) developed by Robert Taylor of the Civil Engineering Department at the University of California at Berkeley, the response of the mix in a repetitive simple shear test at 40°C, using 0.1 sec loading time and a time interval between load applications of 0.6 sec was simulated.
5. A repetitive simple shear test was performed at 40°C for the same conditions as in Step 4.
6. Observed and predicted behaviors were compared.
7. Possible causes of discrepancies were evaluated and corrections needed in the model or in the determination of the material parameters were defined.

Evaluation of the model has been accomplished using a test that was not used to obtain the material parameters and that is of a totally different nature from the tests used to determine the material properties (i.e., the validation test was a repetitive test, whereas the tests used to obtain material properties were either constant rate of loading or sinusoidal in nature). It is important not only to be able to match performance at different stress levels but also at varying rates of loading and unloading.

Specimens for testing were fabricated according to the University of California at Berkeley procedure for rolling wheel compaction (*9*). All specimens of one mix were obtained from the same slab by coring. The cores, 15 cm (6 in.) in diameter by 5 cm (2.5 in.) high, were stored at 20°C before testing.

Determination of Nonlinear Elastic Parameters

To determine the nonlinear elastic parameters, the requisite tests were performed at a temperature of 4°C, which was selected to minimize the viscous response of the mixes. Comparisons between measured and computed results are not included for the mix designated V1T0, since not all of the tests were completed.

Simple Shear Constant Height Test

This test permits the direct determination of three of the nine parameters that define the nonlinear elastic response (i.e., C_2, C_4, and C_9). The test required the use of two hydraulic actuators—one to apply the shear stress to the specimen at a rate of 10 psi/sec; the other, under feedback from an LVDT measuring the relative displacement between the specimen caps, to ensure that constant height is maintained in the specimen (within ±0.00005 in.).

The analysis is based on the assumption that a pure shear state of strain is obtained when $\varepsilon_{12} = \varepsilon_{21} = \varepsilon_0$ and all other strain components are zero. For this situation

$$\sigma_{11} = -C_4 \varepsilon_0^2 \tag{9}$$

$$\sigma_{12} = -C_2 \varepsilon_0 - C_9 \varepsilon_0^3 \tag{10}$$

and

$$\sigma_{33} = -(C_4 + C_5)\varepsilon_0^2 \tag{11}$$

where σ_{11} is the axial stress developed to maintain the height constant and σ_{12} is the shear stress imposed. Unfortunately, σ_{33} cannot be measured; thus, C_5 cannot be directly obtained from the test.

The data in Figure 2 show a typical variation of shear strain with shear stress obtained from a test and that predicted from the model (assuming that the measurements contained no viscous response).

Figure 3 shows the typical variation of axial stresses developed during a test as a function of the shear strain for each of the mixes tested. The most significant aspect of these results is that dilation occurred at 4°C, as evidenced by the compressive stresses in the axial direction necessary to maintain constant height. This suggests that the dilation is strain-related and is associated with the granular structure of dense mixes. Its influence can normally be neglected at low temperatures because the asphalt concrete mix is so stiff that conventional traffic loads are not of sufficient magnitude to generate strains large enough to mobilize the dilation component. At higher temperatures, however, strains sufficient to allow dilation to occur become an important aspect in determining the permanent deformation resistance of a mix.

Figure 3 suggests that the model "captures" the dilation observed in the testing.

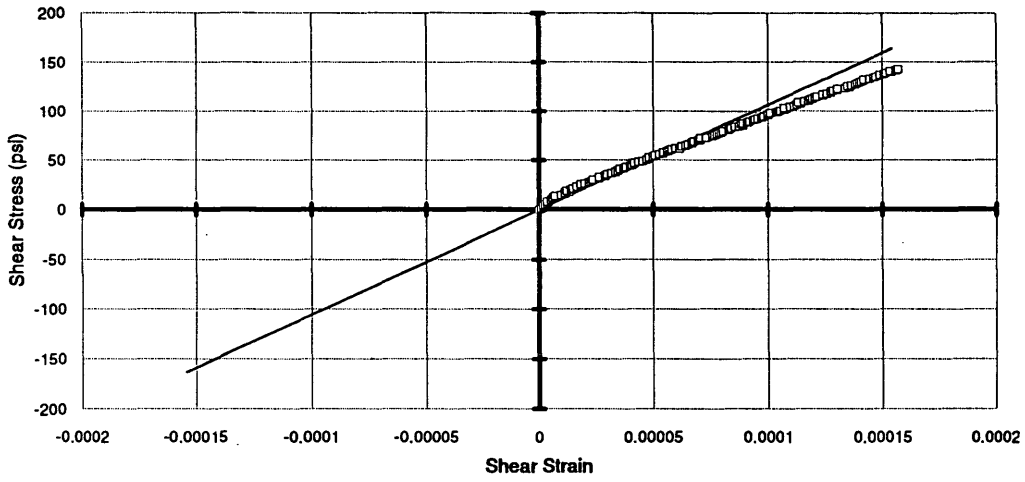

FIGURE 2 Variation of shear stress with shear strain for simple shear tests at 4°C and 10 psi/sec ramping shear stress (model and actual data) (Aggregate RB, Asphalt AAG-1) (V0W0).

Uniaxial Strain Test

The uniaxial strain test permits the direct determination of C_1, C_3, C_6, and C_7 and also provides a check for C_2 and C_4 (obtained from the constant height simple shear test) since the only nonzero strain component is $\varepsilon_{11} = \varepsilon_0$. This assumes that there is no viscous deformation contributing to the response. (If there is viscous deformation, the constant height simple shear and uniaxial strain tests must be executed at the same rate.) In this test the vertical actuator is programmed to ramp the deviatoric axial stress on the sample at a rate of 10 psi/sec while pneumatic servovalves control the confining pressure under feedback from an LVDT measuring the change in perimeter of the specimen. The pneumatic servovalves are programmed to maintain a constant perimeter; thus the change in confining pressure at each instant is just enough to compensate for the bulging of the specimen, ensuring a uniaxial state of strain.

The state of stress is given by

$$\sigma_{11} = C_1 \varepsilon_0 + C_3 \varepsilon_0^2 + C_6 \varepsilon_0^3 \tag{12}$$

and

$$\sigma_{22} = (C_1 + C_2)\varepsilon_0 + (C_3 + C_4)\varepsilon_0^2 + (C_6 + C_7)\varepsilon_0^3 \tag{13}$$

where σ_{11} is the axial stress, σ_{22} is the confining stress, and ε_0 is the axial strain; all other stress components are zero.

Figures 4 and 5 show the typical response of one of the mixes and the best fit obtained with the model parameters.

Figure 6 compares the variation of axial stress with axial strain for the three mixes. Figure 7 compares the variation of the confining stress with the axial strain. In Figure 7 it is interesting to compare the relative performance of the mixes. While the V0W0 mix (Aggregate RB, Asphalt AAG-1, low asphalt content, low voids) only required a confining stress of 17 psi to ensure a state of uniaxial strain, the B1T1 mix (Aggregate RL, Asphalt AAK-1, high asphalt content, high voids) required about 47 psi, even though both were subjected to the same axial stress—approximately 120 psi. This indicated that Mix B1T1 is less stable than Mix V0W0. These results are significant in that they demonstrate that the uniaxial strain test is capable of differentiating between mixes of different stabilities. The Hveem stabilometer would rank the mixes in the same order since that test is similar to the uniaxial strain test.

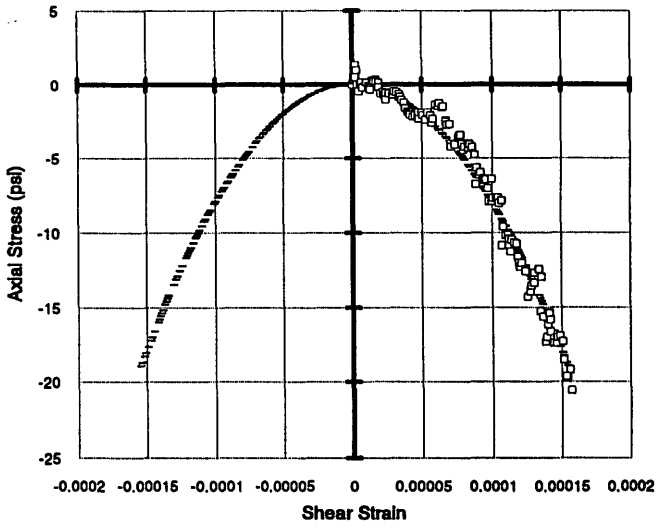

FIGURE 3 Variation of axial stress with shear strain for simple shear tests at 4°C and 10 psi/sec ramping shear stress (model and actual data) (Aggregate RB, Asphalt AAG-1) (V0W0).

Volumetric Test

Results of the volumetric test, together with the constants obtained from the simple shear and uniaxial strain tests, permit the two remaining constants, C_5 and C_8, to be determined. A check of the sum of constants C_1 and C_2 also can be obtained

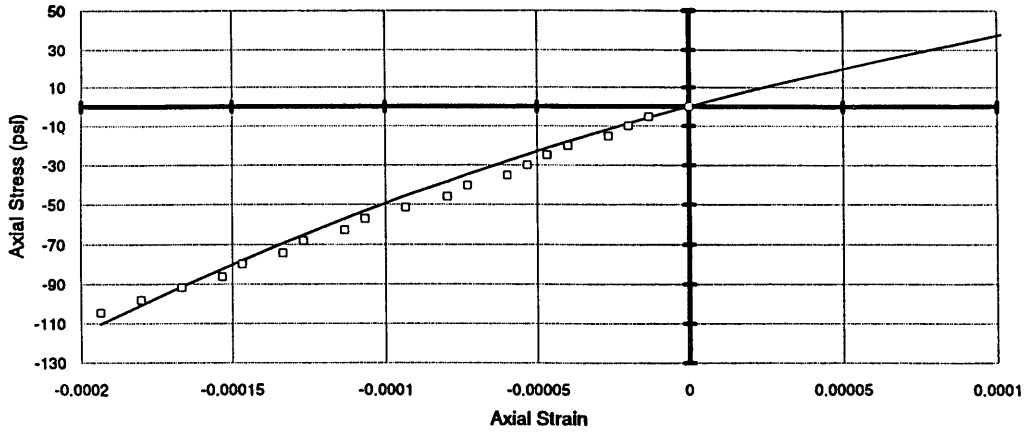

FIGURE 4 Variation of axial stress with axial strain for uniaxial strain tests at 4°C and 10 psi/sec ramping for axial stress (model and actual data) (Aggregate RB, Asphalt AAG-1) (V0W0).

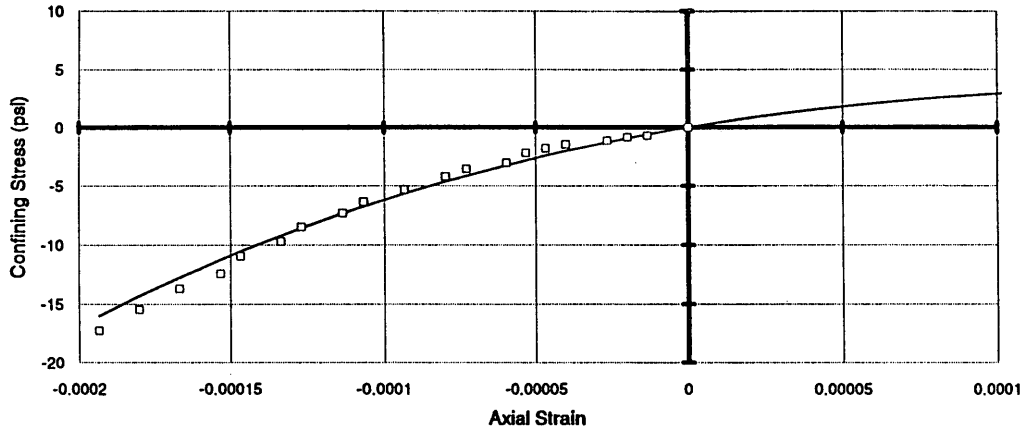

FIGURE 5 Variation of confining stress with axial strain for uniaxial strain tests at 4°C and 10 psi/sec ramping for axial stress (model and actual data) (Aggregate RB, Asphalt AAG-1) (V0W0).

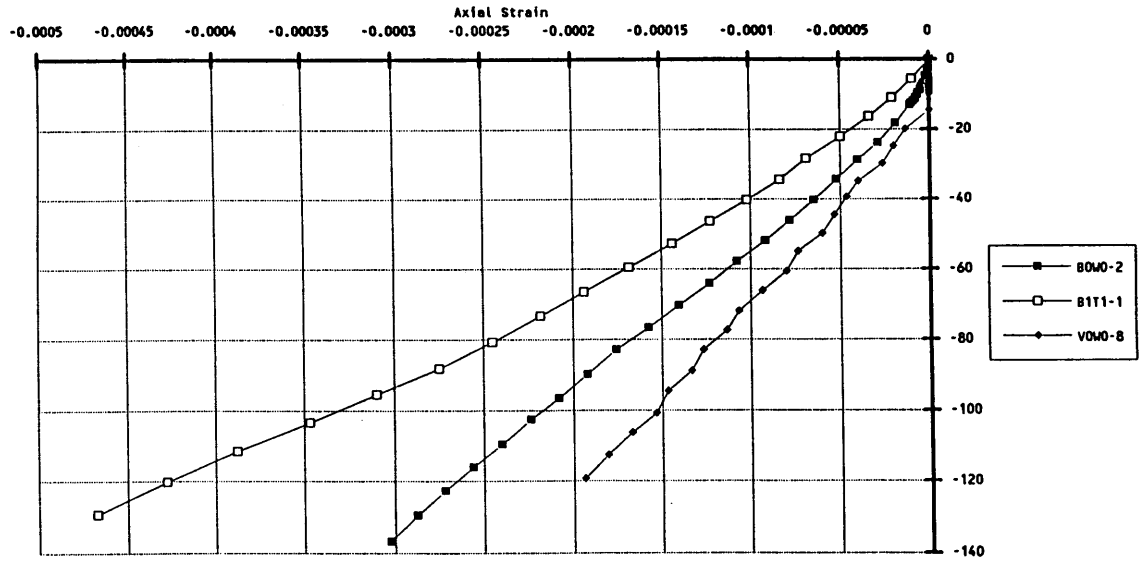

FIGURE 6 Axial stress versus axial strain, uniaxial strain test.

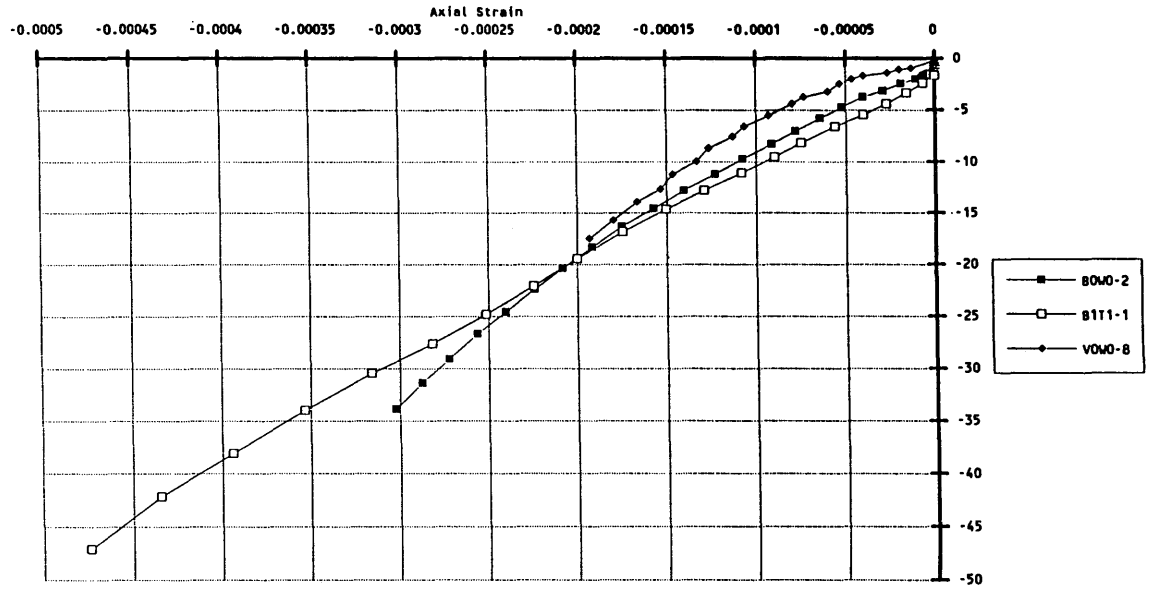

FIGURE 7 Confining stress versus axial strain, uniaxial strain test.

from the volumetric test. In this test the specimen is completely enveloped in a latex membrane and placed inside a pressure cell. The cell pressure is ramped at a rate of 10 psi/sec, and the change in perimeter is measured.

The confining pressure (σ_{22}) and the radial strain ($\varepsilon_0 = \delta/2\pi r$ where δ is the change in perimeter and r is the radius of the specimen) can be computed from the test data. In the volumetric test the state of strain can be stated as $\varepsilon_{11} = \varepsilon_{22} = \varepsilon_{33} = \varepsilon_0$ and the state of stress defined by the following expression:

$$\sigma_{22} = (3C_1 + 2C_2)\varepsilon_0 + (9C_3 + 9C_4 + C_5)\varepsilon_0^2 + (27C_6 + 36C_7 + 4C_8 + 6C_9)\varepsilon_0^3 \quad (14)$$

Figure 8 compares the results obtained from the data with those fitted with the model parameters. Figure 9 compares the response for all four mixes tested.

A summary of the C coefficients obtained from the test results is given in Table 1. All tests were performed at a rate of about 10 psi/sec at 4°C. Whereas that temperature and rate were selected to minimize the viscous deformation, some creep was still present. Accordingly, the C coefficients in Table 1 include some viscous deformation.

The results in Table 1 provide some encouraging comparisons. For example, the values of C_2 and C_4 obtained from the simple shear test for the B0W0 mix compare reasonably well with those obtained from the uniaxial strain test. Also, the value predicted for the coefficient of the linear strain term $(3C_1 + 2C_2)$ in the volumetric test using the values obtained from the uniaxial strain test compares reasonably well with that measured in the volumetric test for all the mixes.

In most instances the comparisons of the C coefficients determined from the tests are reasonable. In the case of C_4 for Mix B1T1, however, a positive value was obtained in the

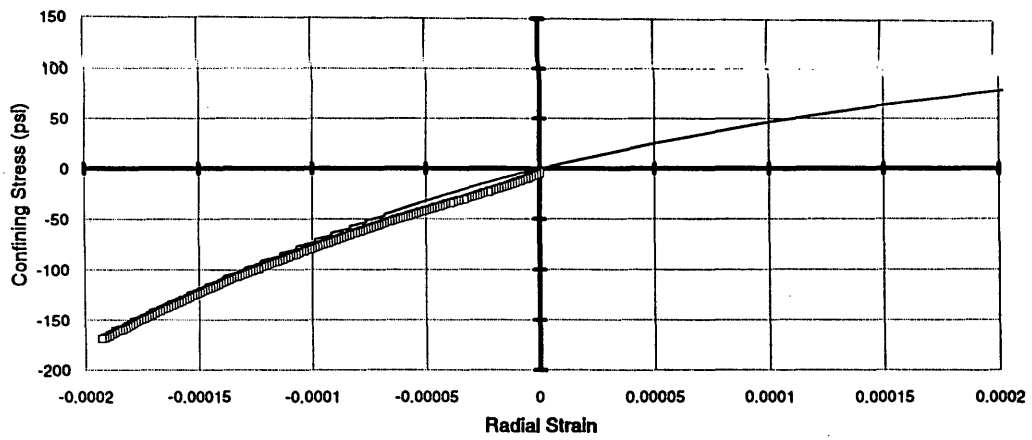

FIGURE 8 Variation of confining stress with radial strain for volumetric tests at 4°C and 15 psi/sec ramping stress (model and actual data) (Aggregate RB, Asphalt AAG-1) (V0W0).

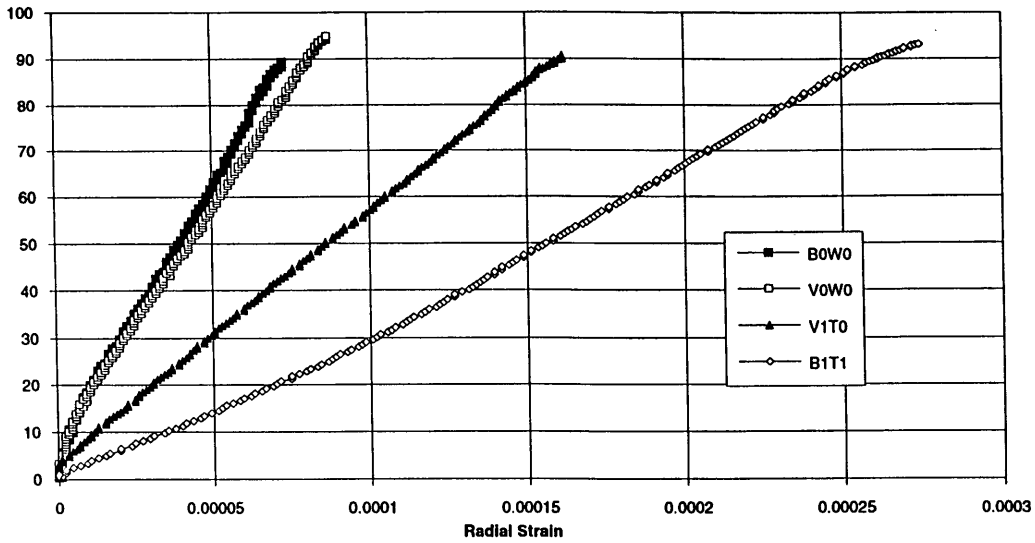

FIGURE 9 Variation of radial strain with confining pressure—volumetric tests.

simple shear test but a negative value was obtained in the uniaxial strain test. Part of this discrepancy might be attributed to the use in the two tests of different specimens whose void contents might have been different.

As stated earlier, some viscous deformations are incorporated in the test data presented herein. Accordingly, the C values are probably smaller than they should be. This has led to the necessity of developing an algorithm that permits determination of the true values for the nonlinear elastic coefficients recognizing that load applications require finite times and are not instantaneous (i.e., values that do not include viscous deformation).

TABLE 1 Summary of C Coefficients Determined from the Simple Shear, Uniaxial Strain, and Volumetric Tests (psi)

		Mix		
		B0W0	V0W0	B1T1
Asphalt type		AAK-1	AAG-1	AAK-1
Asphalt type		RB	RB	RL
Asphalt content (by weight of aggregate)		5.1	4.9	4.3
Compaction method		rolling wheel	rolling wheel	rolling wheel
Air void content (percent)		3.7	3.6	7.9
Simple Shear Test	C_2	-3.88E+05	-1.06E+06	-2.74E+05
	C_4	1.52E+08	7.94E+08	8.14E+07
	C_9	-2.50E+11	-1.00E+10	-2.50E+09
Uniaxial Strain Test	C_1	3.71E+05	4.27E+05	3.11E+05
	C_2	-3.24E+05	-3.83E+05	-2.46E+05
	C_3	-2.94E+08	-6.15E+08	1.39E+07
	C_4	1.17E+08	4.48E+08	-6.84E+07
	C_6	2.91E+11	6.91E+11	-6.73E+10
	C_7	-9.67E+10	-5.01E+11	1.16E+11
Volumetric	C_5	8.97E+08	6.77E+08	8.78E+07
	C_8	-6.50E+11	-6.20E+10	-5.40E+11
From uniaxial strain test:				
$(3C_1 + 2C_2)$		4.66E+05	5.14E+05	4.40E+05
From volumetric test:				
$(3C_1 + 2C_2)$		4.46E+05	5.39E+05	2.52E+05
$(9C_3 + 9C_4 + C_5)$		-6.89E+08	-8.22E+08	-4.03E+08
$(27C_6+36C_7+4C_8+6C_9)$		2.72E+11	3.17E+11	1.65E+11

Determination of Viscous Parameters

The viscous properties of the materials were determined from frequency sweeps at 4°C, 20°C, and 40°C. Strain control shear frequency sweeps were executed at 0.01, 0.02, 0.05, 0.1, 0.2, 0.5, 1, 2, 5, and 10 Hz with an amplitude of 0.0001 in./in. while maintaining the specimen height within ±0.00005 in. Tests were executed from high to low frequency at a particular temperature and from the low temperature to the high temperature.

The imposed sinusoidal strain X at the frequency ω at a strain amplitude X_a,

$$X = X_a \sin(\omega t) \tag{15}$$

will generate a sinusoidal stress P (where t represents time):

$$P = P_a \sin(\omega t + \delta) \tag{16}$$

The complex shear modulus G^* can then be determined as

$$G^* = \frac{P_a}{X_a} \tag{17}$$

At each frequency and temperature, G^* and the phase angle δ were computed from the average of at least three cycles. Using the assumption that the mix is thermorheologically simple, master curves were developed by time-temperature superposition using the IRIS program (*10*). The assumption of a thermorheologically simple response appears reasonable for the small deformations used in the test, as seen in Figure 10.

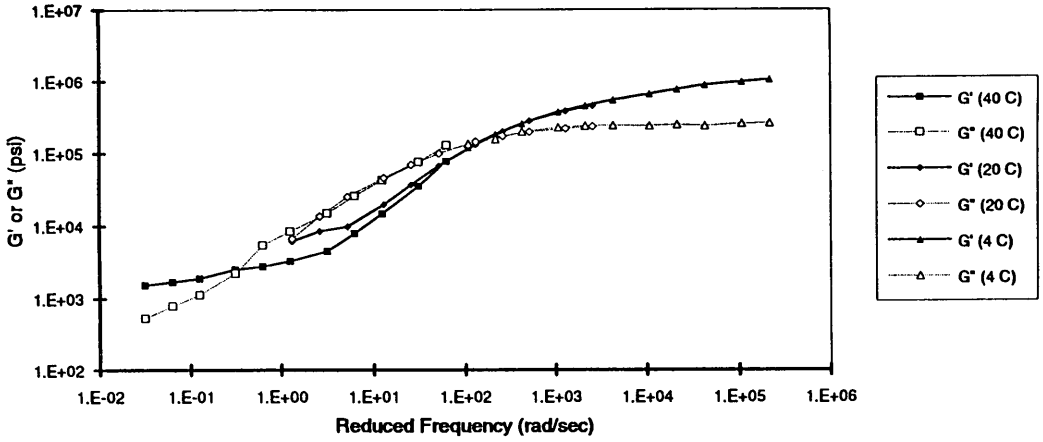

FIGURE 10 Variation of G' and G'' for an asphalt concrete mixture (V0W0) with temperature and frequency. Tests conducted under strain control at 0.0001 shear strain amplitude.

In the determination of the master curve, the C_1 and C_2 coefficients of the WLF equation were also computed:

$$\log a_T = -\frac{C_1(T - T_{ref})}{C_2 + T - T_{ref}} \tag{18}$$

where a_T is the horizontal shift factor and T is the corresponding absolute temperature (degrees Kelvin).

The IRIS program was also used to determine the number (N) of Maxwell elements as well as the values of the constants (g_i and λ_i) required to match the master curves. Table 2 contains the output of IRIS and includes the constants for the WLF equation, which are presented in Table 3. The constants permit the determination of the viscous parameters at any temperature, thus permitting predictions at any pavement temperature.

The N Maxwell elements are defined by their relaxation moduli g_i and their relaxation times λ_i (*11*). Using these values, G' and G'' at any frequency are given by

$$G'(\omega) = G_e + \sum_{i=1}^{N} g_i \frac{(\omega\lambda_i)^2}{1 + (\omega\lambda_i)^2} \tag{19}$$

and

$$G''(\omega) = \sum_{i=1}^{N} g_i \frac{\omega\lambda_i}{1 + (\omega\lambda_i)^2} \tag{20}$$

where G_e is the equilibrium modulus and i refers to the corresponding Maxwell element.

The fitted master curve and the values of G' and G'' obtained from the tests are shown in Figure 11. The results suggest that the assumption of Maxwell elements in parallel represents the dynamic response to a reasonable degree.

The strain control shear frequency sweep test is comparatively easy to perform and provides a reliable measure of the viscous response for a range in temperatures and frequencies at the same strain level. This test may also prove useful in investigating the influence of strain level on the magnitude of the parameters.

To illustrate the influence of asphalt and aggregate type on mix stiffness, variation of $|G^*|$ and phase angle with frequency for four mixes is shown in Figures 12 and 13. The mixes containing Asphalt AAG-1 (V0W0 and V0T1) exhibit different responses from mixes containing Asphalt AAK-1 (B0W0

TABLE 2 Discrete Relaxation Spectra from Computer Program Iris[a]

i	B0W0		V0W0		B1T1		V1T0	
	g_i[b]	λ_i[c]	g_i	λ_i	g_i	λ_i	g_i	λ_i
1	.2489E+07	.1493E-06	.4561E+06	.4763E-05	.2310E+07	.2652E-06	.2676E+06	.2757E-05
2	.2932E+06	.8310E-05	.2565E+06	.4029E-04	.2196E+06	.1240E-04	.2080E+06	.2102E-04
3	.2296E+06	.6178E-04	.2396E+06	.2042E-03	.1949E+06	.7684E-04	.1936E+06	.1144E-03
4	.1314E+-6	.3468E-03	.2482E+06	.1155-02	.1101E+06	.4544E-03	.1818E+06	.6875E-03
5	.8485E+05	.1915E-02	.1439E+06	.5862E-02	.5393E+05	.2643E-02	.1212E+06	.3886E-02
6	.2889E+05	.1064E-01	.7844E+05	.2986E-01	.1694E+05	.1677E-01	.5058E+05	.2087E-01
7	.1929E+05	.4147E-01	.4295E+04	.1758E+00	.2819E+04	.2982E-01	.7978E+04	1037E+00
8	.8068E+04	.3931E+00	.1789E+04	.1199E+01	.4719E+04	.1409E+00	.2923E+04	.8906E+00
9	.2423E+04	.6496E+01	.6061E+03	.1051E+02	.2758E+04	.8117E+00	.5123E+03	.5411E+01
10	.3085E+04	.1859E+03	.1435E+04	.2688E+03	.2085E+04	.5739E+01	.9074E+03	.1698E+04
11					.1240E+04	.1404E+04		

[a]Spectra determination procedure by M. Baumgaertel and H. Winter.
[b]Units of g_i are psi.
[c]Units of λ_i are sec.

TABLE 3 Mix Parameters for Permanent Deformation Model; Three Mixes

MIX TYPE	B0W0		V0W0		B1T1	
Viscous Parameters						
Ref. Temp. (°C)	40		40		40	
C_1 (WLF)	48.02		7.35		53.5	
C_2 (WLF)[K]	-416.57		110.77		583.2	
Viscous Poisson's	0.489		0.489		0.489	
η_0 (psi)	5.94E+05		3.99E+05		1.76E+06	
G_0 (psi)	3.29E+06		1.43E+06		2.92E+06	
α_i	7.57E-01		3.19E-01		7.91E-01	
	8.91E-02		1.79E-01		7.52E-02	
	6.98E-02		1.67E-01		6.68E-02	
	3.99E-02		1.73E-01		3.77E-02	
	2.58E-02		1.01E-01		1.85E-02	
	8.78E-03		5.48E-02		5.80E-03	
	5.86E-03		3.00E-03		9.66E-04	
	2.45E-03		1.25E-03		1.62E-03	
	7.37E-04		4.24E-04		9.45E-04	
	9.38E-04		1.00E-03		7.14E-04	
					4.25E-04	
β_i	6.26E-07		5.45E-06		3.49E-07	
	4.10E-06		2.59E-05		1.55E-06	
	2.39E-05		1.23E-04		8.53E-06	
	7.67E-05		7.19E-04		2.85E-05	
	2.74E-04		2.12E-03		8.12E-05	
	5.18E-04		5.88E-03		1.62E-04	
	1.35E-03		1.89E-03		4.79E-05	
	5.34E-03		5.38E-03		3.79E-04	
	2.65E-02		1.60E-02		1.27E-03	
	9.66E-01		9.68E-01		6.81E-03	
					9.91E-01	
Damage Parameters (Max strain model)						
α_i	0.0003		0.0003		0.0003	
β_i	0.1		0.1		0.1	
n	1		1		1	
Non-Linear Elastic Coefficients		Corrected		Corrected		Corrected
C_1	3.71E+05	7.54E+06	4.27E+05	3.19E+06	3.11E+05	7.37E+06
C_2	-3.24E+05	-6.58E+06	-3.83E+05	-2.86E+06	-2.46E+05	-5.84E+06
C_3	-2.94E+08		-6.15E+08		1.39E+07	
C_4	1.17E+08		4.48E_08		-6.84E+07	
C_5	8.97E+08		6.77E+08		8.78E+07	
C_6	2.91E+11		6.91E+11		-6.73E+10	
C_7	-9.67E+10		-5.01E+11		1.16E+11	
C_8	-6.50E+11		-6.20E+10		-5.40E+11	
C_9	-2.50E+11		-1.00E+10		-2.50E+09	

and B1T1) relative to phase angle variation, as shown in Figure 13. At lower frequencies (higher temperatures) the mixes with Aggregate RB exhibit higher stiffnesses than the mixes with RL material. At higher frequencies the influence of the asphalt (stiffness) predominates.

Determination of Damage Parameters

Damage parameters were estimated from tests performed at 20°C and 1 Hz. Strain control shear tests were executed with strain amplitudes of 0.0001, 0.0002, 0.0005, 0.001, and 0.002 in./in. to investigate the influence of strain level on damage (the specimen height was maintained constant within ±0.00005 in.). In this analysis it was assumed that only 1 Maxwell element out of the 10 or 12 usually obtained from the IRIS program would be significantly influenced for the frequency and temperature used.

The material properties were computed as presented in Equations 15, 16, and 17. Furthermore, the viscosity, η, of the dashpot was computed by

$$\eta = \frac{G''(1 + \tan\delta)}{\omega \tan\delta} \tag{21}$$

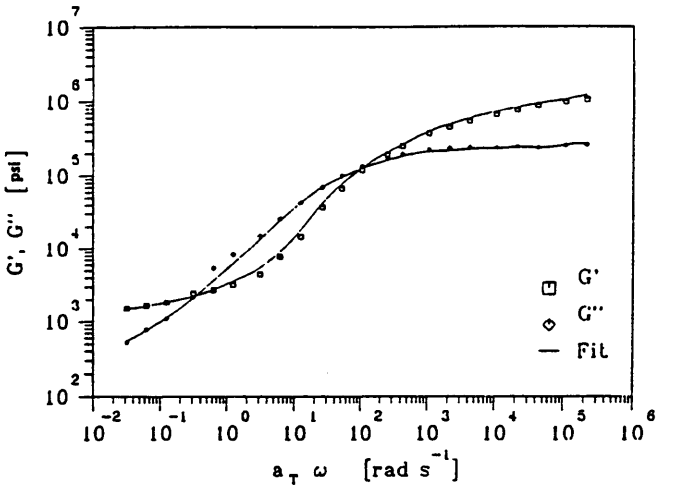

FIGURE 11 Variation of G' and G'' with frequency for Mix V0W0 (Aggregate RB, Asphalt AAG-1) at a reference temperature of 40°C.

where

G'' = loss modulus,
ω = test frequency (rad/sec), and
δ = phase angle.

The stiffness, E, of the spring is given by

$$E = \eta \tan\delta \tag{22}$$

Figure 14 shows the variation of stiffness ratio (stiffness at any strain amplitude divided by stiffness at small strain amplitude) with strain magnitude. It appears that the strain amplitude has comparatively small influence in reducing the spring stiffness, although slight strain softening is observed.

Figure 15 suggests that the dashpot viscosity is strongly influenced by strain amplitude. In this figure the ratio of the viscosity at any strain amplitude to that of a strain level of 0.0001 in./in. is plotted as a function of strain amplitude. Moreover, when the ordinate, termed damage, has a value of 1, the dashpot is considered undamaged. As the value of

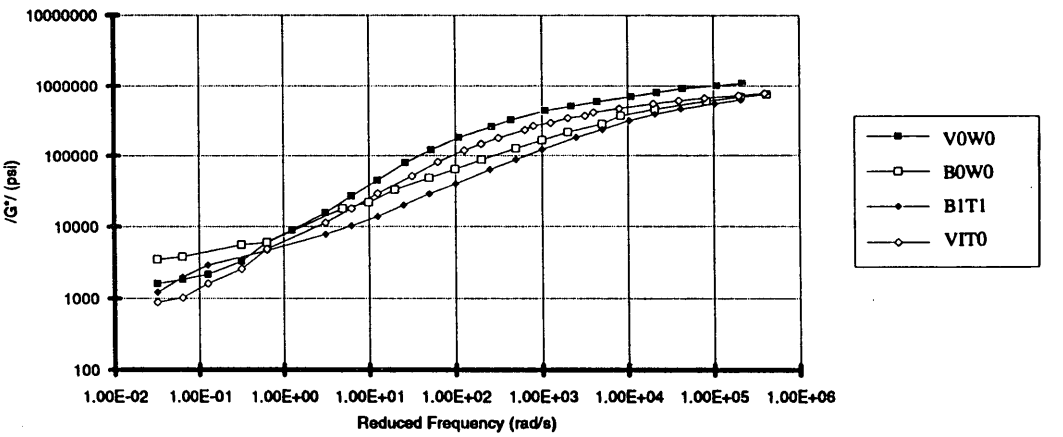

FIGURE 12 Complex shear modulus versus reduced frequency (rad/sec) (40°C reference) from shear frequency sweeps.

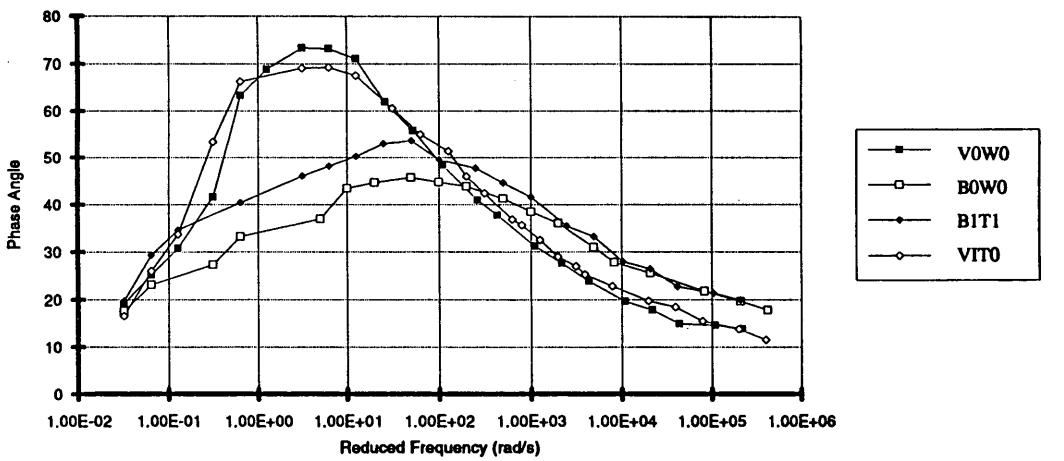

FIGURE 13 Phase angle versus reduced frequency (40°C reference) for shear frequency sweeps.

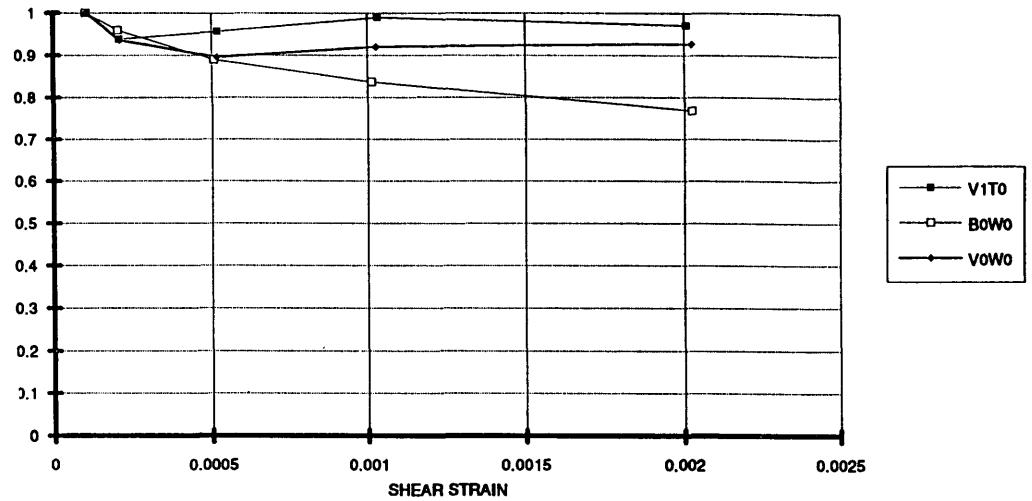

FIGURE 14 Variation of stiffness ratio (E/E_0) with strain amplitude in strain sweep tests at 20°C and 1 Hz.

the ordinate decreases (i.e., approaches 0), the damage to the dashpot increases.

The development of damage with strain level obtained from creep tests is also shown in Figure 15. The variation of the damage parameter with strain magnitude appears to follow a similar path for both strain sweeps and creep tests. The results strongly suggest a highly nonlinear behavior in the dashpots; however, the nonlinearity seems to be independent of the mix.

Material Properties

Table 3 contains a summary of the material properties obtained for three of the four mixes. The values of G_0 represent the instantaneous shear moduli obtained from the IRIS program. The values of C_2 ($C_2 = -2G_0$) obtained from the frequency sweeps (see "corrected" column) are higher than those obtained from the simple shear tests, uniaxial strain tests, and volumetric tests. This is not surprising since the shear frequency sweeps performed at 4°C and 10 Hz yield higher values of G^* than those obtained at 0.1 Hz at the same temperature. Thus it is apparent that the tests conducted at 4°C to determine the nonlinear elastic parameters contain a viscous component.

To match the viscous parameters and the C constants, the C_1 and C_2 values were corrected proportionally. The other C values were not corrected. This fact makes the analysis more linear because the contribution of the nonlinear terms is slightly minimized.

A program to determine all the nonlinear elastic, viscous, and damage parameters, taking each of these factors into consideration by using an iterative procedure with a quadratic convergence, is under development and should rapidly yield consistent and accurate parameters.

The data in Table 3 (using the larger values for C_1 and C_2) provide the basis for predicting the performance of the mixes in some other form of loading and thus serve to provide validation of the permanent deformation model.

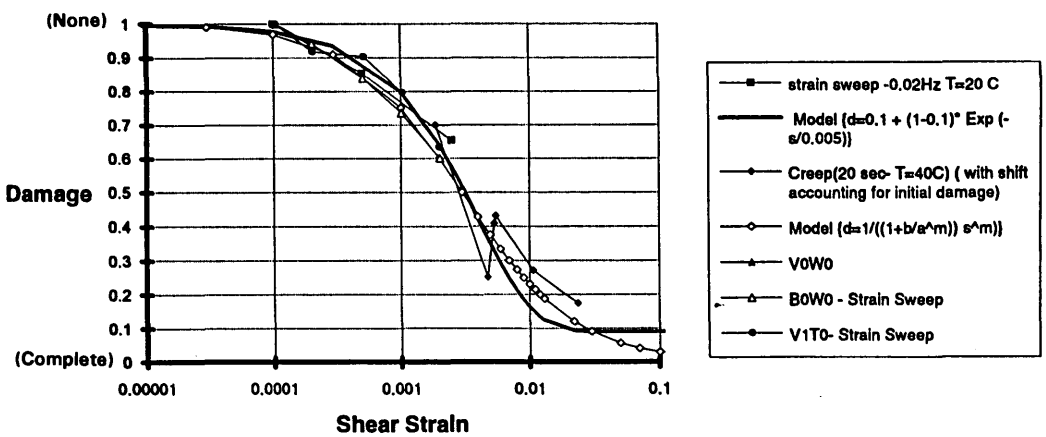

FIGURE 15 Comparison of the shape of the damage function obtained from shear strain sweeps and shear creep tests with a proposed damage model.

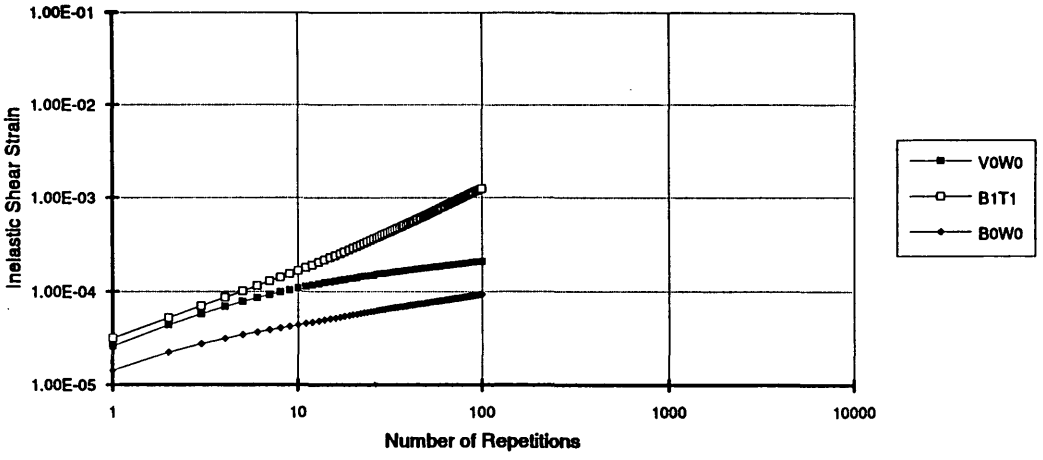

FIGURE 16 Model prediction for accumulation of permanent deformation in the repetitive-load simple shear test.

VALIDATION

A repetitive simple shear test at constant height was selected for validation. This test was conducted at 40°C using a time of loading of 0.1 sec and a time interval between load applications of 0.6 sec. The magnitude of the repetitive shear stress was 7.5 psi. The height of each specimen was maintained within ±0.00005 in.

For validation purposes, a two-element finite element mesh representing half of the cylindrical specimen was used to take advantage of the antisymmetry of the load. The model assumes that the states of stress in the true specimen is perfect (i.e., that a state of pure shear stress exists within the cylindrical specimen).

Using this model and the maerial properties presented in Table 3, 100 cycles of 0.1 sec loading and 0.6 sec unloading were simulated (Figure 16). The simulations accurately ranked the mixes according to their known permanent deformation resistance. This was an important demonstration considering that the mix properties used in the simulations were based on measurements not only at different loading rates but also from totally different types of tests.

Figure 17 compares results obtained from the test of the V0W0 mix with the prediction obtained from the model assuming several levels of damage. Adding a damage component to the mix model significantly improves the ability to accurately simulate test measurements. A relatively good fit between measured and simulated response can be obtained when mix damage is accounted for.

PAVEMENT SECTION EXAMPLE

To illustrate the implementation of the approach outlined in Figure 1, an example of the use of the finite element program is presented. Figure 18 shows a finite element mesh created to represent half of a full-depth, one-lane pavement section. In this simplified two-dimensional model, the loads have been simulated as continuous loading strips consistent with the plane strain assumption. (A full three-dimensional model could have

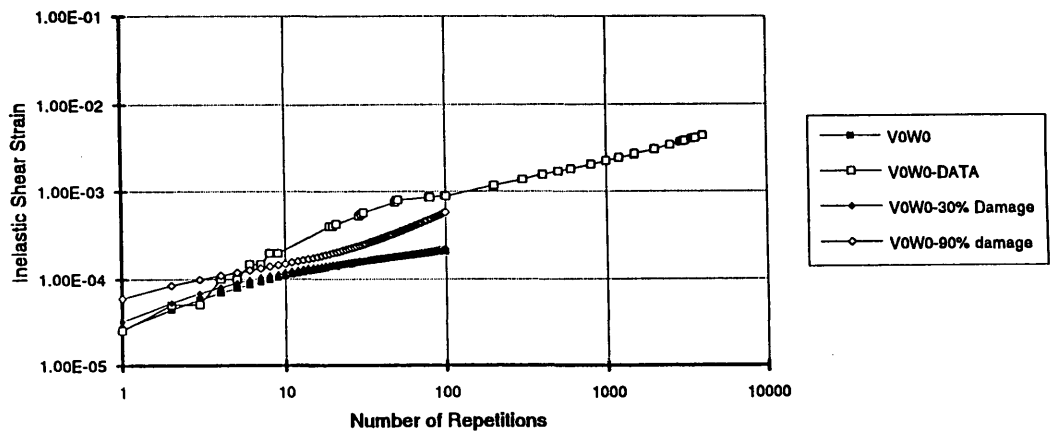

FIGURE 17 Comparison between data and model prediction of accumulation of permanent deformation in the repetitive-load simple shear test.

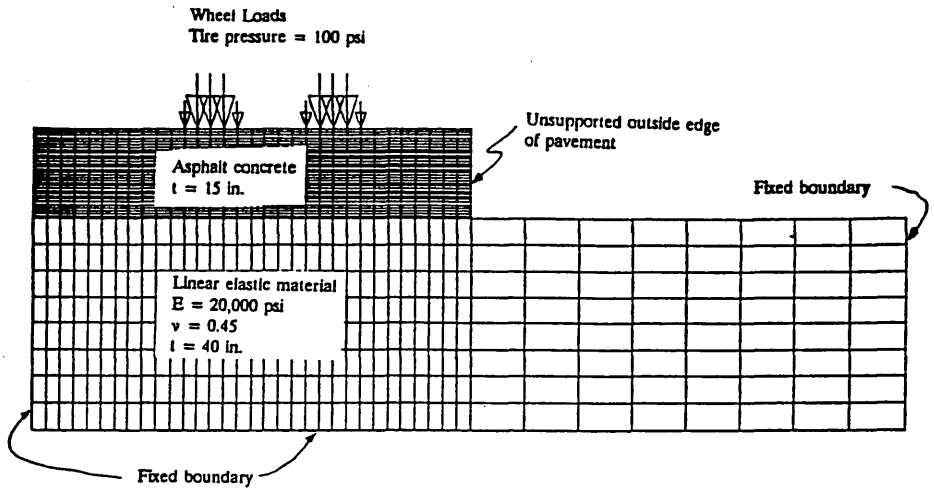

FIGURE 18 Two-dimensional mesh representing a cross section of a pavement section.

been formulated, but because of limited computer resources at the time such a solution could not have been implemented.)

To rapidly achieve significant levels of permanent deformation on the asphalt concrete layer with very few load applications, the material properties used were significantly weakened by reducing the magnitude of both the C constant and the viscous parameters. Moreover, a repetitive haversine load with a 0.3-sec loading time and 0.4-sec rest between load application was used to simulate very slow-moving traffic. The magnitude of the load was selected as 500 psi to increase even more the rate of accumulation of permanent deformation.

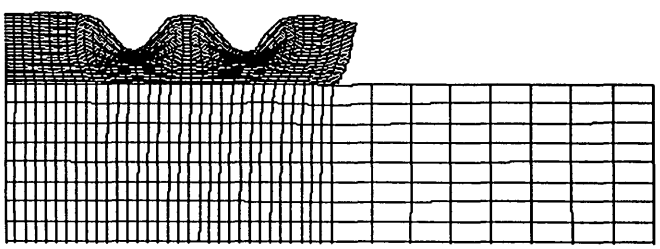

FIGURE 19 Deformed shape of the pavement section after five cycles.

The FEAP program running on an IBM-RS6000 was used. The total cpu time to reach five cycles was about 5 hr. This time could be significantly reduced by using a slightly coarser mesh (without compromising the accuracy of the results) and by increasing the magnitude of the small time steps used to prevent divergence due to such high loads (with tire pressures of 100 psi, the magnitude of the time steps could be increased).

Figure 19 shows the deformed shape at the end of the fifth cycle magnified 100 times. The figure shows the permanently deformed shape without the load being applied. The variation of the pavement profile at the end of the first, second, and fifth cycles is presented in Figure 20. The upheavals due to the shear flow and dilation are similar to those encountered in rutted pavement sections.

This example illustrates the capability of the model to analyze boundary value problems representative of pavement structures and to simulate the general shape of the permanent deformation profile of rutted pavement.

SUMMARY

A nonlinear elastic viscous with damage model for asphalt-aggregate mixes has been proposed. The model is based on

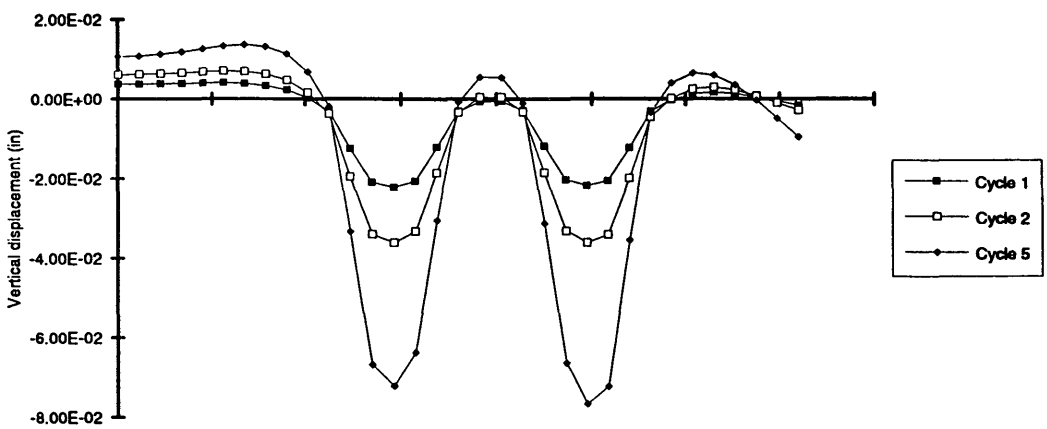

FIGURE 20 Variation of pavement profile with the number of load application, stress level 500 psi, 0.3-sec loading time, 0.4-sec rest period.

principles of mechanics and is directly amenable to finite element approximations.

A new series of tests (i.e., uniaxial strain test, simple shear test at constant height, and volumetric test) has been developed to determine the nonlinear elastic material properties. Simple shear frequency and strain sweep tests at constant height were introduced to determine the viscous and damage parameters for the model.

Results indicate that the model is capable of capturing the most important aspects of the permanent deformation response of asphalt-aggregate mixes. The tests selected for determination of the material parameters were found to be easy to conduct and to yield consistent material properties.

Material properties, obtained for three of the four mixes that had the complete battery of tests performed, were used in simulations that reasonably ranked the mixes according to their known permanent deformation resistance. In this procedure the evaluation of the model behavior was made through a test from which no material parameters were obtained and that is of a totally different nature from those used to determine the material properties (i.e., the validation test was a repetitive test, whereas the tests used to obtain material properties used either a constant rate of loading or were sinusoidal in nature). This was an important demonstration, considering that the mix properties used in the simulations were based on measurements not only at different frequencies and times of loading but from totally different types of tests and stress levels.

Manual determination of material properties from test measurements is a tedious, time-consuming process. A program is being developed to determine requisite properties with minimum user intervention. As a result, testing at 4°C in an effort to minimize the viscous component of the mix response is no longer considered necessary, and standard testing will now be performed at more convenient temperatures and loading rates (e.g., 40°C). Also, as a result of this exercise, a fourth temperature, 60°C, has been added to the frequency sweep tests for some mixes to ensure that the range in loading times required to simulate response is bounded.

Efforts are also being made to refine the model to incorporate a measure of damage capable of capturing inelastic permanent deformation not fully explained by viscous behavior.

The development of a constitutive law for asphalt concrete behavior that can be used in three-dimensional finite element programs is very important to the development of a procedure to accurately predict the permanent deformation response of pavements subjected to moving traffic. For example, tire contact pressures, which vary significantly with tire type and inflation pressure, have a significant influence on the development of permanent deformation. We believe that it is necessary to use a three-dimensional program to properly reflect such effects. The type of model proposed herein can be used in such a finite element idealization.

ACKNOWLEDGMENTS

The work reported herein has been conducted as a part of SHRP Project A-003A. SHRP, a unit of the National Research Council, was authorized by Section 128 of the Surface Transportation and Uniform Relocation Assistance Act of 1987. This project is titled Performance-Related Testing and Measuring of Asphalt-Aggregate Interactions and Mixtures and is being conducted by the Institute of Transportation Studies, University of California, Berkeley. Carl L. Monismith is Principal Investigator. The support and encouragement of Rita B. Leahy of SHRP is gratefully acknowledged.

Special thanks are also due to John Harvey for his efforts in preparing the specimens and editing for publication and to Maggie Paul for the manuscript preparation.

REFERENCES

1. J. B. Sousa, J. Craus, and C. L. Monismith. *Summary Report on Permanent Deformation in Asphalt Concrete*. Report SHRP-A/IR-91-104. Strategic Highway Research Program, Washington, D.C., 1991.
2. A. Tayebali, J. Goodrich, J. B. Sousa, and C. L. Monismith. Relationships Between Modified Asphalt Binders Rheology and Binder-Aggregate Pavement Deformation Response. *Asphalt Paving Technology*, Vol. 60, 1991, pp. 121–159.
3. J. B. Sousa, J. A. Deacon, and C. L. Monismith. Effect of Laboratory Compaction Method on Permanent Deformation Characteristics of Asphalt Concrete Mixtures. *Asphalt Paving Technology*, Vol. 60,. 1991, pp. 533–587.
4. H. S. Papazian. *The Response of Linear Viscoelastic Material in Frequency Domain*. Dissertation. Report 172-2. Transportation Engineering Center, Ohio State University, Columbus, Ohio, Dec. 1961.
5. I. J. Lubliner. *On the Thermodynamic Foundations of Non-linear Solid Mechanics*. Vol. 54, 1972, pp. 259–278.
6. Marsden and Hughes. *Mathematical Foundation of Elasticity*. Prentice-Hall, Englewood Cliffs, N.J., 1983.
7. W. Flugge. *Visoelasticity*. Springer-Verlag, Berlin, 1975.
8. J. M. Gibb, P. S. Pell, and S. F. Brown. *An Evaluation of the Wheel-Tracking Test as a Means of Assessing Resistance to Permanent Deformation*. SWK Pavement Engineering Ltd., Sept. 1991.
9. J. B. Sousa, J. Harvey, L. Painter, J. A. Deacon, and C. L. Monismith. *Evaluation of Laboratory Procedures for Compacting Asphalt-Aggregate Mixtures*. TM-UCB-A-003A-90-5. Institute of Transporation Studies, University of California, Berkeley, 1991.
10. M. Baumgaertel, P. R. Soskey, and H. H. Winter. *IRIS (Innovation Rheological Interface Software)*. User's manual, 1990.
11. M. Baumgaertel and H. H. Winter. Determination of Discrete Relaxation and Retardation Time Spectra from Dynamic Mechanical Data. *Rheologica Acta*, Vol. 28, 1989, pp. 511–519.